

Journal of Organometallic Chemistry, 363 (1989) 45–60
Elsevier Sequoia S.A., Lausanne – Printed in The Netherlands
JOM 09451

The structure of 2,2-di-*t*-butyl-1,3,2-dioxa-, -oxathia-, and -dithia-stannolanes: a study by solution and solid state NMR and single crystal X-ray diffraction

Paul A. Bates, Michael B. Hursthouse

Chemistry Department, Queen Mary College, Mile End Road, London, E1 4NS (Great Britain)

Alwyn G. Davies * and Seán D. Slater

Chemistry Department, University College London, 20 Gordon Street, London WC1H 0AJ (Great Britain)

(Received August 1st, 1988)

Abstract

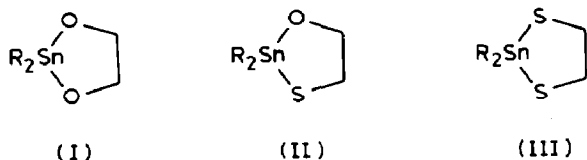
X-Ray diffraction shows that 2,2-di-*t*-butyl-1,3,2-dioxastannolane exists as a 5-coordinate dimer. The corresponding oxathiastannolane is similarly dimerised through oxygen, but in the crystalline phase the dithiastannolane is a 4-coordinate monomer.

Comparison of the $^{117/119}\text{Sn}$ NMR spectra of the compounds as solids and in solution shows that in solution, the dioxastannolane retains its dimeric structure, but the dimeric oxathiastannolane is in equilibrium with the monomer, and the dithiastannolane is a simple monomer.

Introduction

Whereas tetraalkyltin(IV) compounds R_4Sn are simply tetrahedrally 4-coordinate in all physical states, organotin compounds containing electronegative ligands, $\text{R}_n\text{SnX}_{4-n}$, undergo self-association to a degree which may increase in the sequence gas phase < solution < solid [1,2]. These structures have been extensively investigated by a wide variety of techniques including particularly $^{119\text{m}}\text{Sn}$ Mössbauer spectroscopy [3,4], and ^{119}Sn NMR spectroscopy in solution [5,6] and the solid state, by reference to data from an increasing number of single crystal X-ray diffraction studies [7].

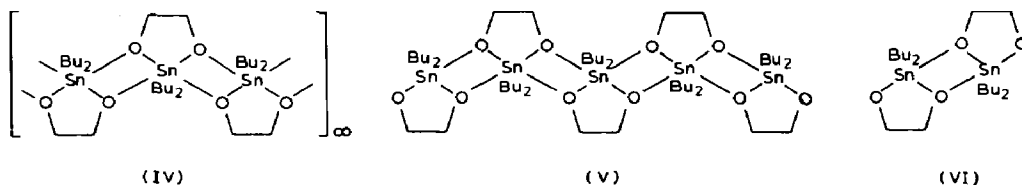
In this context we have been particularly interested [8] in the dialkyldioxastannolanes (I) [9], dialkyloxathiastannolanes (II) [10], and dialkyldithiastannolanes (III) [11]. These compounds are particularly susceptible to association, probably because the change from 4- to 5- or 6-coordination relieves strain in the 5-membered ring.



These studies have emphasised how the different degrees of association of these compounds are controlled not only by the electronegativity of the chalcogenide ligands (O or S), but also by their sizes and shapes.

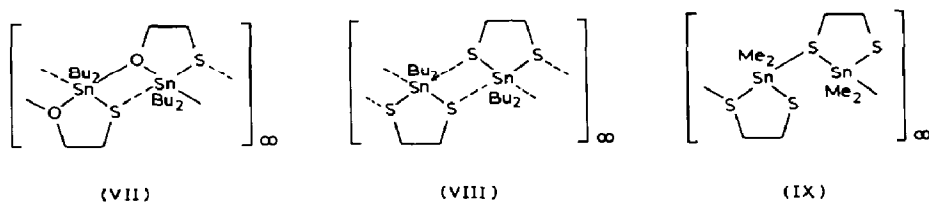
Less attention has been paid in this series of compounds to the steric effect of the alkyl group R. In this paper we focus attention on the steric effect of the *t*-butyl group as a ligand, and we have made particular use of the techniques of solution and solid state $^{117/119}\text{Sn}$ NMR spectroscopy, and of single crystal X-ray diffraction.

The present position regarding the compounds (I), (II), and (III) is as follows.



2,2-Di-*n*-butyl-1,3,2-dioxastannolane itself (I, R = *n*-Bu) in solution exists principally as a dimer (VI) but in the crystal it is a 6-coordinate infinite polymer (IV) [9]. The corresponding di-*n*-butyltin derivative of methyl 4,6-di-*O*-benzylidene- α -D-mannopyranoside in the crystal exists as a pentamer (V) [12], and the corresponding glucopyranoside is a dimer (VI) [13]. These differences in the solid state structures can be rationalised in terms of the bulk of the pyranose moieties [9].

2,2-Di-*n*-butyl-1,3,2-oxathiastannolane (II, R = *n*-Bu), like the corresponding dioxastannolane, is dimeric in solution, but in the crystal it exists as a linear 5-coordinate oxygen-bridged polymer (VII), with probably some further weak S-Sn interaction [10].



2,2-Di-*n*-butyl-1,3,2-dithiastannolane (III, R = *n*-Bu) on the other hand is monomeric in solution, and in the crystal these monomeric molecules are weakly symmetrically bonded to neighbouring molecules as shown in (VIII) [11]. Dimethyl-dithiastannolane (III, R = Me) however in the solid state consists of a linear 5-coordinate polymer (IX) [14,15].

Results

2,2-Di-*t*-butyl-1,3,2-dioxastannolane (I, R = Bu^t) and 2,2-di-*t*-butyl-1,3,2-oxathiastannolane (II, R = Bu^t) were prepared by the azeotropic dehydration of

Table 1

Mössbauer spectra of di-*t*-butyl-dioxa-, -oxathia-, and -dithia-stannolanes ^a

	δ (mm s ⁻¹)	ΔE_q (mm s ⁻¹)
$\text{Bu}^t_2\text{SnOCH}_2\text{CH}_2\text{O}$	1.36	2.55
$\text{Bu}^t_2\text{SnOCH}_2\text{CH}_2\text{S}$	1.46	2.36
$\text{Bu}^t_2\text{SnSCH}_2\text{CH}_2\text{S}$	1.64	1.96

^a At 88 K, with reference to SnO₂.

di-*t*-butyltin oxide with ethane-1,2-diol or 2-mercaptoethanol respectively. 2,2-Di-*t*-butyl-1,3,2-dithiastannolane (III, R = Bu^t) was obtained by heating together di-*t*-butyltin oxide and dimethyl-1,3,2-dithiastannolane in toluene.

The ^{119m}Sn Mössbauer chemical shifts and quadrupole coupling constants for the three compounds are given in Table 1, and the data from the solution and solid state ¹³C and ^{117/119}Sn NMR spectra in Table 2. The solid state ¹¹⁷Sn NMR spectra are illustrated in Fig. 1, 3, and 5, and the structures as determined by single crystal X-ray diffraction are shown in Fig. 2, 4, and 6 respectively. Bond lengths and interbond angles are listed in Tables 3, 4, and 5 respectively.

Table 2

Solution and solid state NMR spectra of $\text{Bu}^t_2\text{SnOCH}_2\text{CH}_2\text{O}$, $\text{Bu}^t_2\text{SnOCH}_2\text{CH}_2\text{S}$, and $\text{Bu}^t_2\text{SnSCH}_2\text{CH}_2\text{S}$

	Solution	Solid
$\text{Bu}^t_2\text{SnOCH}_2\text{CH}_2\text{O}$		
$\delta(^{117/119}\text{Sn})^a$	-225	-225 ^b
$^2J(^{117}\text{Sn}-^{119}\text{Sn})/\text{Hz}$	206	-
$\delta(^{13}\text{C}(\text{CH}_3)_3)$	41.6	42.5
$\delta(\text{C}^{13}\text{CH}_3)_3)$	30.7	31.5
$\delta(\text{O}^{13}\text{CH}_2)$	64.0 and 67.4	65.7 and 68.6
$\text{Bu}^t_2\text{SnOCH}_2\text{CH}_2\text{S}$		
$\delta(^{117/119}\text{Sn})^a$	-25(0.45 M) +52(0.02 M)	-96 and -101 ^b
$\delta(^{13}\text{C}(\text{CH}_3)_3)$	42.6	42.8 and 43.1
$\delta(\text{C}^{13}\text{CH}_3)_3)$	30.6	31.1 and 31.8
$\delta(\text{O}^{13}\text{CH}_2)$	69.0	69.4 (br)
$\delta(\text{S}^{13}\text{CH}_2)$	32.2	-
$\text{Bu}^t_2\text{SnSCH}_2\text{CH}_2\text{S}$		
$\delta(^{117/119}\text{Sn})^a$	+171	+171 ^b
$\delta(^{13}\text{C}(\text{CH}_3)_3)$	38.1	38.1 and 38.4
$\delta(\text{C}^{13}\text{CH}_3)_3)$	30.5	32.0
$\delta(\text{S}^{13}\text{CH}_2)$	36.5	33.0 and 32.2

^a The observed nucleus was ¹¹⁹Sn in solution, but ¹¹⁷Sn in the solid state (see Experimental).^b The anisotropic parameters were as follows:

	Anis.	Asymm.	σ_{11}	σ_{22}	δ_{33}
$\text{Bu}^t_2\text{SnOCH}_2\text{CH}_2\text{O}$	473	1.10	-555	-209	90
$\text{Bu}^t_2\text{SnOCH}_2\text{CH}_2\text{S}$	333	1.48	-373	-43	125
	311	1.85	-396	-13	106
$\text{Bu}^t_2\text{SnSCH}_2\text{CH}_2\text{S}$	39	2.89	121	195	196

Discussion

2,2-Di-t-butyl-1,3,2-dioxastannolane

Di-t-butyl-dioxastannolane exists in the crystal as a dimer containing 5-coordinate tin in a severely distorted trigonal bipyramidal configuration (Fig. 2). The tin and oxygen atoms lie on a crystallographic mirror plane, and the two halves of the molecule are related by a two-fold rotation axis passing perpendicularly through the centre of the SnOSnO ring.

The carbon atoms of the OCH₂CH₂O ring are disordered half each way to either side of the mirror plane.

This contrasts with the structure of di-n-butyl-dioxastannolane (IV) which exists in the crystal as a 6-coordinate ribbon polymer, but it is very similar to the structure of the glycopyranoside (VI), where the glucoside moiety in (VI) exerts the same function as the t-butyl groups in (II, R = Bu^t) in sterically preventing association beyond the stage of a dimer.

In the solid state NMR spectrum (Table 2 and Fig. 1), these tin atoms show a single resonance at δ 224.7, and the non-equivalent methylene groups in the dioxastannolane rings show separate ¹³C signals at 65.7 and 68.6.

In solution, the dioxastannolane shows ¹¹⁹Sn and ¹³C signals which differ from the solid state values by no more than might be ascribed to change of medium. In particular, the ¹¹⁹Sn chemical shift, which would be most susceptible to a change in coordination number is the same as that in the solid state. The resonance is now narrow enough to show ¹¹⁹Sn-¹¹⁷Sn coupling to the second tin atom in the ring.

We conclude that in solution, the dioxastannolane has the same structure (Fig. 2) as it has in the crystal.

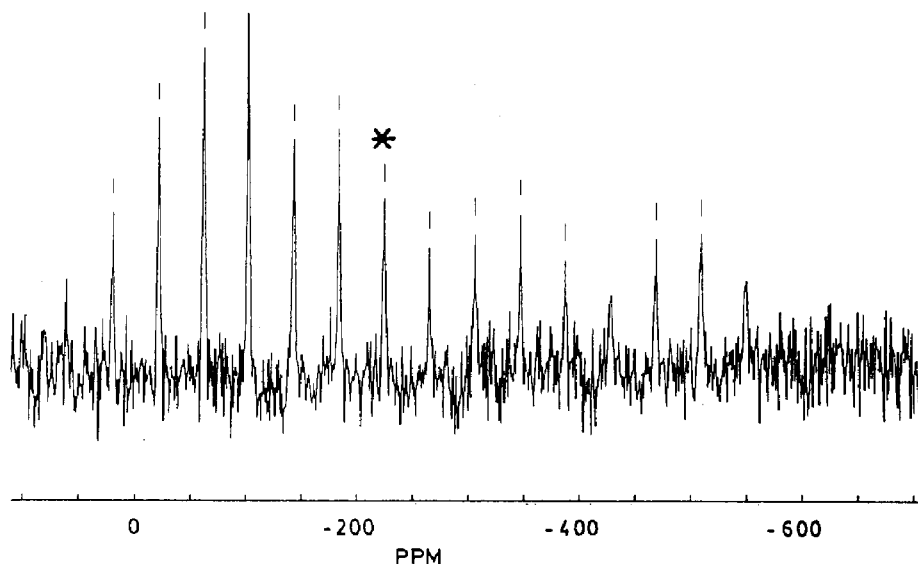


Fig. 1. Solid State ¹¹⁷Sn NMR spectrum of 2,2-di-t-butyl-1,3,2-dioxastannolane.

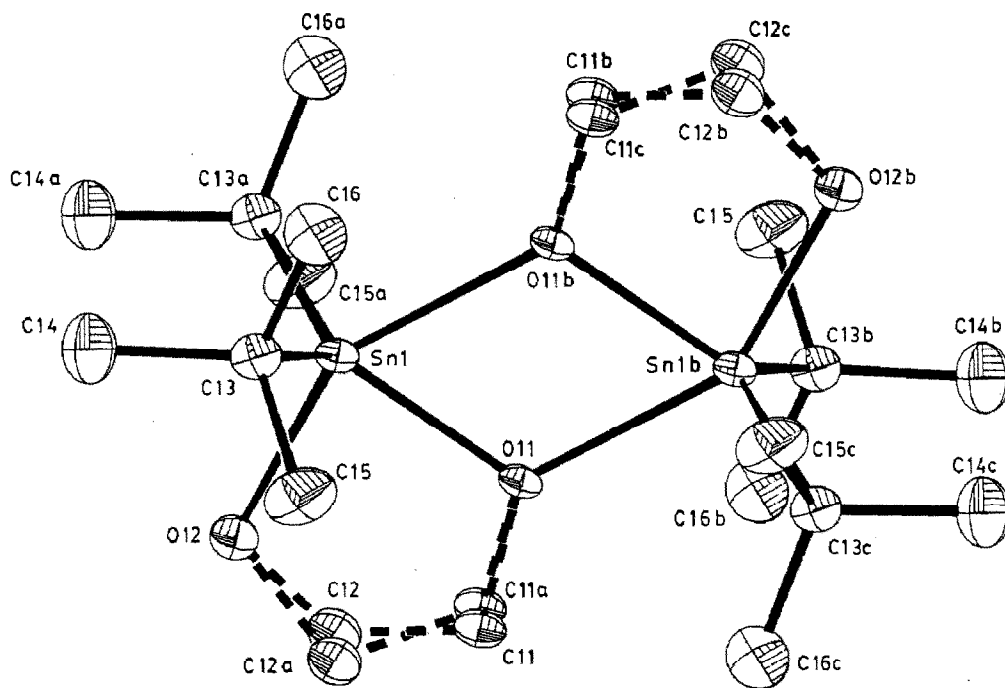


Fig. 2. Molecular structure of 2,2-di-*t*-butyl-1,3,2-dioxastannolane for one of the two independent molecules. Key to symmetry operations relating designated atoms to reference atoms at (x, y, z) : (a) $x, y, -z$. (b) $1.0 - x, 1.0 - y, -z$. (c) $1.0 - x, 1.0 - y, z$.

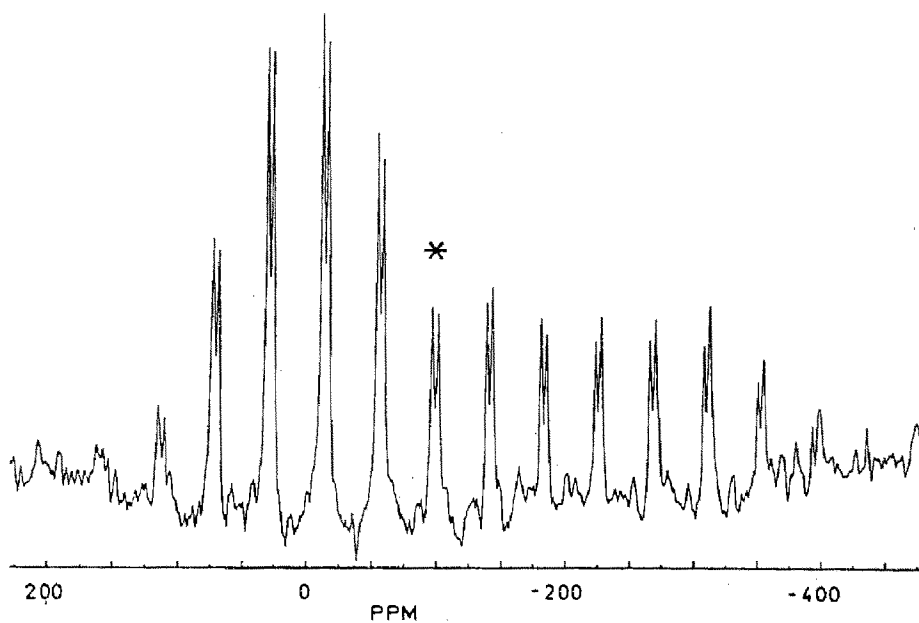


Fig. 3. Solid state ^{117}Sn NMR spectrum of 2,2-di-*t*-butyl-1,3,2-oxathiastannolane.

Table 3

Bond lengths (Å) and angles (°) for $[\text{Bu}^t_2\text{SnOCH}_2\text{CH}_2\text{O}]_2$

<i>(i) Molecule 1</i>			
O(11)–Sn(1)	2.086(6)	O(12)–Sn(1)	2.049(7)
O(11b)–Sn(1)	2.253(7)	C(13)–Sn(1)	2.188(7)
C(11)–O(11)	1.449(9)	C(12)–O(12)	1.479(12)
C(12)–C(11)	1.514(15)	C(14)–C(13)	1.521(9)
C(15)–C(13)	1.517(9)	C(16)–C(13)	1.506(10)
<i>(ii) Molecule 2^a</i>			
O(21)–Sn(2)	2.090(7)	O(22)–Sn(2)	2.047(7)
O(21e)–Sn(2)	2.244(7)	C(23)–Sn(2)	2.184(7)
C(21)–O(21)	1.442(9)	C(22)–O(22)	1.475(12)
C(22)–C(21)	1.505(15)	C(24)–C(23)	1.514(10)
C(25)–C(23)	1.535(9)	C(26)–C(23)	1.512(9)
<i>(i) Molecule 1</i>			
O(11b)–Sn(1)–O(11)	67.3(3)	O(12)–Sn(1)–O(11)	79.7(3)
O(12)–Sn(1)–O(11b)	147.2(2)	C(13)–Sn(1)–O(11)	117.3(2)
C(13)–Sn(1)–O(11b)	97.5(3)	C(13)–Sn(1)–O(12)	97.5(2)
C(13a)–Sn(1)–C(13)	125.0(5)	Sn(1b)–O(11)–Sn(1)	112.7(3)
C(11)–O(11)–Sn(1)	111.8(5)	C(11)–O(11)–Sn(1b)	133.9(5)
C(12)–O(12)–Sn(1)	112.5(5)	C(12)–C(11)–O(11)	108.1(8)
C(11)–C(12)–O(12)	105.8(8)	C(14)–C(13)–Sn(1)	107.3(5)
C(15)–C(13)–Sn(1)	108.1(4)	C(15)–C(13)–C(14)	108.9(6)
C(16)–C(13)–Sn(1)	112.4(5)	C(16)–C(13)–C(14)	109.6(6)
C(16)–C(13)–C(15)	110.4(6)		
<i>(ii) Molecule 2^a</i>			
O(21e)–Sn(2)–O(21)	67.7(4)	C(22)–Sn(2)–O(21)	79.7(3)
O(22)–Sn(2)–O(21e)	147.4(3)	C(23)–Sn(2)–O(21)	117.4(2)
C(23)–Sn(2)–O(21e)	97.5(4)	C(23)–Sn(2)–O(22)	97.4(3)
C(23d)–Sn(2)–C(23)	124.9(5)	Sn(2e)–O(21)–Sn(2)	112.3(3)
C(21)–O(21)–Sn(2)	113.1(5)	C(21)–O(21)–Sn(2e)	133.3(5)
C(22)–O(22)–Sn(2)	110.8(5)	C(22)–C(23)–O(21)	106.1(8)
C(25)–C(23)–Sn(2)	108.0(8)	C(24)–C(23)–Sn(2)	107.0(5)
C(26)–C(23)–Sn(2)	108.1(5)	C(25)–C(23)–C(24)	108.6(6)
C(26)–C(23)–C(25)	112.9(4)	C(26)–C(23)–C(24)	110.3(6)
C(26)–C(23)–C(25)	109.7(6)		

key to symmetry operations relating designated atoms to reference atoms at (x, y, z):

- (a) x, y, –z
 (b) 1.0 – x, 1.0 – y, –z
 (d) x, y, 1.0 – z
 (e) 1.0 – x, –y, 1.0 – z

^a There are two independent, but chemically equivalent, molecules. For the atom labelling scheme of molecule 2, the first digit of each corresponding label for molecule 1 is changed from 1 to 2.

2,2-Di-*t*-butyl-1,3,2-oxathiastannolane

The oxathiastannolane in the crystal (Fig. 4) forms a dimer through oxygen to give a structure with many general features in common with that of the dioxastannolane, but the sulphur atoms are slightly displaced from the SnOSnO plane, there is no C_{2v} axis, the *t*-butyl groups are no longer exactly equivalent, and there is no disorder of the carbon atoms in the oxathiastannolane rings.

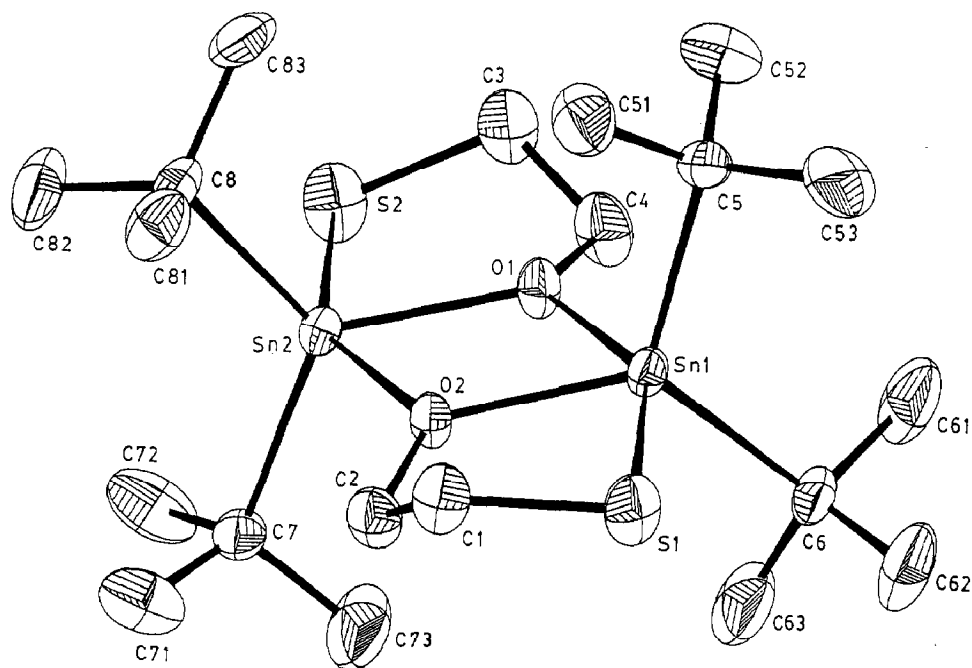


Fig. 4. Molecular structure of 2,2-di-*t*-butyl-1,3,2-oxathiastannolane.

The ^{117}Sn NMR spectrum in the solid state (Table 2), shows two slightly non-equivalent tin sites at $\delta -96$ and -101 , and the profile of the spinning side bands (Fig. 3) reflecting the individual values of the anisotropic chemical shifts, is similar to that for the dioxastannolane (Fig. 1). The ^{13}C NMR spectrum similarly shows the presence of two slightly non-equivalent *t*-butyl groups. The ^{13}C chemical shift of the CH_2O group (69.4) is close to that in the dioxastannolane, but the ^{13}C of the CH_2S group, which would be expected to appear at about $\delta 32$, could not be detected; perhaps it is obscured by the signal due to the methyl groups at $\delta 31.1$ and 31.8 .

The ^{119}Sn NMR spectrum recorded on a CDCl_3 solution is substantially different. At a concentration of 0.45 M the tin resonance is at -25 ppm, but it moves downfield as the solution is diluted, and at 0.02 M the signal appears at $+52$ ppm. Clearly in solution, the 5-coordinate dimeric oxathiastannolane dissociates to give the 4-coordinate monomer. As the power of the oxygen as a Lewis base will probably be similar in the dioxastannolane and the oxathiastannolane, it appears that the presence of the sulphur ligand in the oxathiastannolane must weaken the Lewis acidity of the tin, reducing the stability of the dimer.

2,2-Di-t-butyl-1,3,2-dithiastannolane

We have shown previously that dioxastannolanes will react with dialkyltin oxides to give initially 1/1 adducts [16]. The reaction of dimethyldithiastannolane with di-*t*-butyltin oxide to give di-*t*-butyldithiastannolane may be envisaged as following a similar mechanism, the insertion reaction being followed by the elimination of the very stable dimethyltin oxide (equation 1).

(Continued on p. 54)

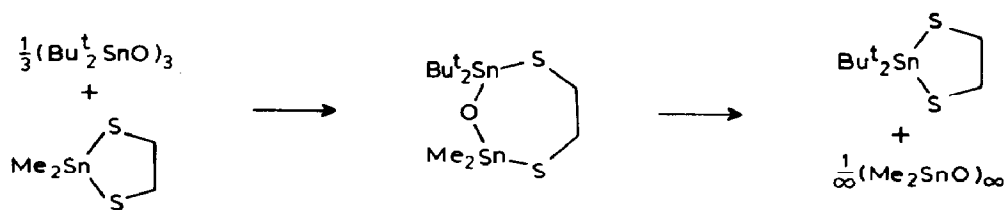


Table 4

Bond lengths (Å) and angles (°) for $[\text{Bu}_2^t\text{SnOCH}_2\text{CH}_2\text{S}]_2$

S(1)–Sn(1)	2.492(3)	O(1)–Sn(1)	2.297(5)
O(2)–Sn(1)	2.079(5)	C(5)–Sn(1)	2.202(7)
C(6)–Sn(1)	2.207(7)	S(2)–Sn(2)	2.494(3)
O(1)–Sn(2)	2.084(5)	O(2)–Sn(2)	2.291(5)
C(7)–Sn(2)	2.213(7)	C(8)–Sn(2)	2.202(7)
C(1)–S(1)	1.796(8)	C(3)–S(2)	1.818(8)
C(4)–O(1)	1.455(6)	C(2)–O(2)	1.443(6)
C(2)–C(1)	1.484(8)	C(4)–C(3)	1.477(9)
C(51)–C(5)	1.538(10)	C(52)–C(5)	1.497(9)
C(53)–C(5)	1.489(9)	C(61)–C(6)	1.507(10)
C(62)–C(6)	1.534(11)	C(63)–C(6)	1.493(10)
C(71)–C(7)	1.509(11)	C(72)–C(7)	1.500(11)
C(73)–C(7)	1.429(11)	C(81)–C(8)	1.527(9)
C(82)–C(8)	1.494(9)	C(83)–C(8)	1.523(10)
O(1)–Sn(1)–S(1)	149.0(1)	O(2)–Sn(1)–S(1)	82.2(2)
O(2)–Sn(1)–O(1)	66.9(2)	C(5)–Sn(1)–S(1)	100.5(2)
C(5)–Sn(1)–O(1)	95.5(2)	C(5)–Sn(1)–O(2)	117.1(3)
C(6)–Sn(1)–S(1)	99.5(2)	C(6)–Sn(1)–O(1)	95.7(3)
C(6)–Sn(1)–O(2)	122.8(3)	C(6)–Sn(1)–C(5)	118.7(3)
O(1)–Sn(2)–S(2)	82.6(2)	O(2)–Sn(2)–S(2)	149.6(1)
O(2)–Sn(2)–O(1)	67.0(2)	C(7)–Sn(2)–S(2)	99.0(3)
C(7)–Sn(2)–O(1)	121.3(3)	C(7)–Sn(2)–O(2)	96.3(3)
C(8)–Sn(2)–S(2)	97.8(2)	C(8)–Sn(2)–O(1)	117.2(3)
C(8)–Sn(2)–O(2)	96.7(2)	C(8)–Sn(2)–C(7)	120.6(3)
C(1)–S(1)–Sn(1)	94.1(2)	C(3)–S(2)–Sn(2)	93.9(3)
Sn(2)–O(1)–Sn(1)	112.8(2)	C(4)–O(1)–Sn(1)	129.0(4)
C(4)–O(1)–Sn(2)	117.6(4)	Sn(2)–O(2)–Sn(1)	113.2(2)
C(2)–O(2)–Sn(1)	118.3(4)	C(2)–O(2)–Sn(2)	127.8(4)
C(2)–C(1)–S(1)	111.4(5)	C(1)–C(2)–O(2)	111.4(5)
C(4)–C(3)–S(2)	111.2(5)	C(3)–C(4)–O(1)	111.7(5)
C(51)–C(5)–Sn(1)	107.2(5)	C(52)–C(5)–Sn(1)	114.4(5)
C(52)–C(5)–C(51)	108.1(7)	C(53)–C(5)–Sn(1)	107.0(5)
C(53)–C(5)–C(51)	108.8(7)	C(53)–C(5)–C(52)	111.2(7)
C(61)–C(6)–Sn(1)	110.4(5)	C(62)–C(6)–Sn(1)	107.6(5)
C(62)–C(6)–C(61)	107.4(7)	C(63)–C(6)–Sn(1)	109.4(5)
C(63)–C(6)–C(61)	112.4(7)	C(63)–C(6)–C(62)	109.5(7)
C(71)–C(7)–Sn(2)	110.7(5)	C(72)–C(7)–Sn(2)	107.9(5)
C(72)–C(7)–C(71)	106.9(7)	C(73)–C(7)–Sn(2)	110.2(5)
C(73)–C(7)–C(71)	108.8(9)	C(73)–C(7)–C(72)	112.3(9)
C(81)–C(8)–Sn(2)	112.0(5)	C(82)–C(8)–Sn(2)	105.7(5)
C(82)–C(8)–C(81)	112.2(6)	C(83)–C(8)–Sn(2)	108.7(5)
C(83)–C(8)–C(81)	106.8(6)	C(83)–C(8)–C(82)	111.4(6)

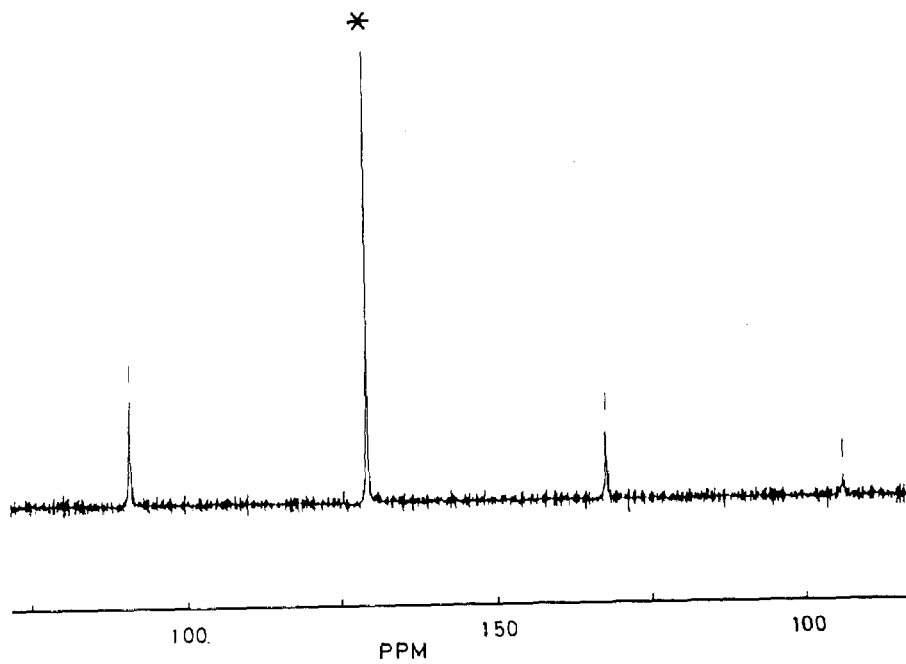


Fig. 5. Solid state ^{117}Sn NMR spectrum of 2,2-di-t-butyl-1,3,2-dithiastannolane.

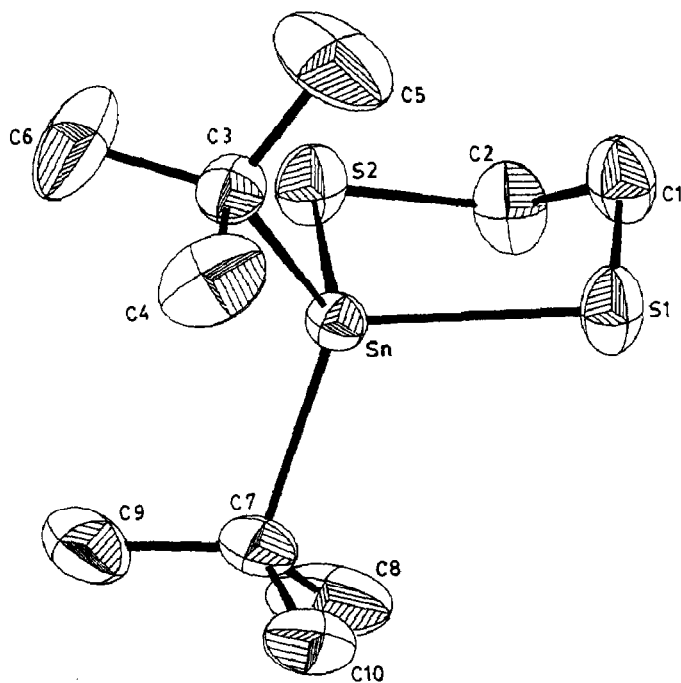


Fig. 6. Molecular structure of 2,2-di-t-butyl-1,3,2-dithiastannolane.

Table 5

Bond lengths (Å) and angles (°) for $\text{Bu}^t_2\text{SnSCH}_2\text{CH}_2\text{S}$

S(1)–Sn	2.411(3)	S(2)–Sn	2.417(3)
C(3)–Sn	2.184(7)	C(7)–Sn	2.173(6)
C(1)–S(1)	1.816(6)	C(2)–S(2)	1.821(7)
C(2)–C(1)	1.495(7)	C(4)–C(3)	1.501(10)
C(5)–C(3)	1.493(8)	C(6)–C(3)	1.492(9)
C(8)–C(7)	1.518(9)	C(9)–C(7)	1.504(9)
C(10)–C(7)	1.521(9)		
S(2)–Sn–S(1)	92.2(1)	C(3)–Sn–S(1)	114.7(2)
C(3)–Sn–S(2)	108.0(2)	C(7)–Sn–S(1)	110.6(2)
C(7)–Sn–S(2)	109.5(2)	C(7)–Sn–C(3)	118.5(3)
C(1)–S(1)–Sn	95.9(3)	C(2)–S(2)–Sn	95.6(2)
C(2)–C(1)–S(1)	115.5(5)	C(1)–C(2)–S(2)	113.5(5)
C(4)–C(3)–Sn	110.5(5)	C(5)–C(3)–Sn	108.2(5)
C(5)–C(3)–C(4)	109.5(6)	C(6)–C(3)–Sn	108.8(5)
C(6)–C(3)–C(4)	107.0(7)	C(6)–C(3)–C(5)	112.8(8)
C(8)–C(7)–Sn	107.1(5)	C(9)–C(7)–Sn	108.7(4)
C(9)–C(7)–C(8)	110.1(6)	C(10)–C(7)–Sn	110.1(4)
C(10)–C(7)–C(8)	110.1(6)	C(10)–C(7)–C(9)	110.7(6)

In the crystal, di-*t*-butyldithiastannolane exists as monomeric units with distorted tetrahedral geometry of the four ligands about the tin (Fig. 6). The S–Sn–S angle within the ring is 92.6°, and the C–Sn–C angle is 118.0°. The *t*-butyl groups are slightly non-equivalent, and the ring adopts a half-chair conformation.

The closest intermolecular Sn–S approach is 6.43 Å, much greater than the sum of the van der Waals radii (ca. 4.0 Å).

This monomeric character of the dithiastannolane in the solid state is reflected in the Mössbauer quadrupole splitting parameter (ΔE_q) (Table 1) which is smaller than that in the dioxa- and oxathiastannolanes.

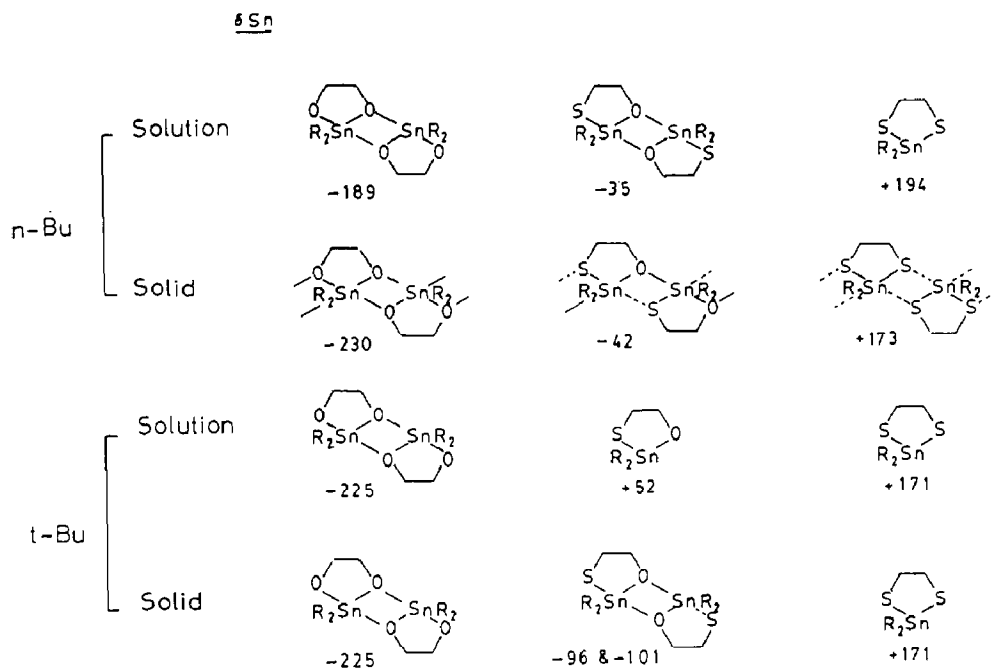
The ^{13}C , and particularly the $^{117/119}\text{Sn}$ NMR chemical shifts in the solid state are very close to those in solution, as would be expected for a compound which does not undergo further association on solidification.

This structure of the di-*t*-butyl-dithiastannolane contrasts with those of the dimethyl and di-*n*-butyl analogues which are strongly 5-coordinate [14,15] or weakly 6-coordinate [11] respectively.

Conclusion

The influence of the nature of the ligand (O or S), of the alkyl groups (*n*-butyl or *t*-butyl) and of the phase (solution or crystalline solid), and the correlation with the $^{117/119}\text{Sn}$ chemical shifts, is shown in Scheme 1, which illustrates the following points.

The *n*-butyl compounds are all more highly associated in the solid state than in solution, whereas the *t*-butyl compounds show little tendency to associate further when they solidify. This difference must result principally from the steric bulk of the *t*-butyl group. In the oxathiastannolane this results in the di-*n*-butyl compound



Scheme 1.

existing in the solid state as a 5-coordinate polymer, but the di-*t*-butyl compound as a 5-coordinate dimer.

Oxygen has a stronger coordinating power than sulphur; this is shown by the fact that oxathiastannolanes associate through oxygen.

Oxygen ligands enhance the Lewis acidity of tin more than do sulphur ligands. This is indicated by the fact that in solution, di-*t*-butyldioxastannolane is more strongly associated (through oxygen) than di-*t*-butyloxathiastannolane.

The studies have emphasised the power of the NMR technique for determining organotin structures in the solid state. The $^{117/119}\text{Sn}$ chemical shift is particularly sensitive to slight variations in the ligation of the tin atom; when the Sn chemical shift is the same in solution and the solid state, the nature and degree of association can be taken to be the same under both conditions, and the structure elucidated by X-ray crystallography can be assumed to apply equally well in solution.

Experimental

NMR Spectra

^{119}Sn NMR spectra of organotin compounds in solution were recorded on a Varian XL200 instrument, and ^{13}C and ^{117}Sn spectra of solids on the University of London Intercollegiate Research Service MSL300 instrument at Royal Holloway and Bedford New College. The ^{117}Sn resonance frequency (109.940 MHz) was chosen because interference was picked up on the ^{119}Sn resonance frequency (111.914 MHz) from the communication system from the nearby Heathrow airport. The solid state NMR spectra were recorded using magic angle spinning, high power

decoupling, and cross polarization under the typical conditions of a spinning rate of 3800–4500 Hz, 200–500 transients, 1–10 μ s contact time, and a 10s pulse delay.

Tin chemical shifts are relative to $\delta(\text{Me}_4\text{Sn}) = 0$, and calibrated against $(\text{Me}_3\text{Sn})_4\text{C}$, $\delta + 48.2$.

Mössbauer spectra

Mössbauer spectra were recorded on the ULIRS instrument at Birkbeck College. Samples were cooled in liquid nitrogen, and isomer shifts are quoted relative to SnO_2 .

Table 6

Crystal data, details of intensity measurements and structure refinement for $[\text{Bu}^t_2\text{SnOCH}_2\text{CH}_2\text{O}]_2$, $[\text{Bu}^t_2\text{SnOCH}_2\text{CH}_2\text{S}]_2$, and $\text{Bu}^t_2\text{SnSCH}_2\text{CH}_2\text{S}$

Formule	$\text{C}_{20}\text{H}_{44}\text{O}_4\text{Sn}$	$\text{C}_{20}\text{H}_{44}\text{O}_2\text{S}_2\text{Sn}_2$	$\text{C}_{10}\text{H}_{22}\text{S}_2\text{Sn}$
<i>M</i>	585.95	618.07	443.78
Crystal system	Orthorhombic	Monoclinic	Monoclinic
Space group	<i>Pbam</i>	<i>P2₁/n</i>	<i>P2₁/n</i>
<i>a</i> (Å)	12.444(1)	11.505(6)	6.500(2)
<i>b</i> (Å)	12.544(1)	14.943(3)	13.747(2)
<i>c</i> (Å)	16.286(1)	16.202(7)	16.612(2)
β (°)		103.23(4)	92.31(2)
<i>U</i> (Å ³)	2542.2(4)	2711(2)	1482.6(4)
<i>Z</i>	4	4	4
<i>D_c</i> (g cm ⁻³)	1.531	1.514	1.988
<i>F</i> (000)	1184	1248	856
Crystal size/mm	0.28 × 0.23 × 0.20	0.63 × 0.60 × 0.50	0.75 × 0.26 × 0.25
μ (cm ⁻¹)	19.91	20.09	36.25
Absorption corr. (min., max.)	89%, 100%	88%, 100%	84%, 100%
2 θ -range	3.0, 50.0	3.0, 50.0	3.0, 50.0
<i>h, k, l</i> range	0 → 14, 0 → 14, 0 → 19	0 → 13, 0 → 17, -19 → 19	0 → 7, 0 → 16, -19 → 19
Intensity variation	< 3%	< 3%	< 3%
Total no. of reflections	2544	5245	2865
No. of unique reflections	2323	4778	2611
Significance test	$F_o > 6.0\sigma(F_o)$	$F_o > 6.0\sigma(F_o)$	$F_o > 6.0\sigma(F_o)$
No. of reflections used in the refinement	1769	4353	2072
No. of refined parameters	163	271	136
Max. least-squares shift-to-error ratio	0.08	0.20	0.07
Min. and Max. height in final difference			
Fourier map, $\Delta\rho$ (\bar{e} Å ⁻³)	-0.69, 0.75	-1.12, 0.78	-0.41, 0.71
Function minimized	$\sum w(F_o - F_c)^2$	$\sum w(F_o + F_c)^2$	$\sum w(F_o - F_c)^2$
Weighting scheme parameter <i>g</i> in $w = 1/[\sigma^2(F_o) + gF_o^2]$	0.001	0.002	0.0003
Final <i>R</i>	0.029	0.033	0.029
Final <i>R_w</i>	0.033	0.044	0.032

2,2-Di-*t*-butyl-1,3,2-dioxastannolane

A mixture of equimolar amounts (8×10^{-3} mol) of di-*t*-butyltin oxide and ethane-1,2-diol in toluene (120 cm^3) was heated under reflux for 4 h under a Dean and Stark water separator. The solution was filtered, concentrated to one third of its volume, and set aside at -18°C , when the dioxastannolane crystallised out. It was recrystallised from toluene; m.p. 224°C (decomp.). Found: C, 41.0; H, 7.61. $\text{C}_{10}\text{H}_{22}\text{O}_2\text{Sn}$ calcd.: C, 41.0; H, 7.5%. $\delta(^1\text{H})$ (CDCl_3 , 60 MHz) 1.40 (s, 18H, Me), $^3J(^{119}\text{Sn}-\text{H})$ 104 Hz, $^3J(^{117}\text{Sn}-\text{H})$ 99 Hz; 3.76 (s, 4H, CH_2O), $^3J(^{117/119}\text{Sn}-\text{H})$ 29 Hz. ^{13}C And $^{117/119}\text{Sn}$ spectra are described in Table 2.

2,2-Di-*t*-butyl-1,3,2-oxathiastannolane

A mixture of di-*t*-butyltin oxide and 2-mercaptoethanol in toluene was dehydrated azeotropically to give the oxathiastannolane, m.p. $158.5\text{--}159.5^\circ \text{C}$ (from toluene). Found: C, 39.0; H, 6.94; S, 10.5. $\text{C}_{10}\text{H}_{22}\text{OSSn}$ calcd.: C, 38.9; H, 7.17; S, 10.4%. $\delta(^1\text{H})$ (CDCl_3 , 200 MHz) 1.37 (s, 18H, Me), $^3J(^{119}\text{Sn}-\text{H})$ 100.3 Hz, $^3J(^{117}\text{Sn}-\text{H})$ 96.0 Hz; 2.75 (t, 2H, CH_2S), $^3J(\text{H}-\text{H})$ 5.2 Hz, $^3J(^{117/119}\text{Sn}-\text{H})$ 18.5 Hz; 3.95 (t, 2H, CH_2O), $^3J(^{117/119}\text{Sn}-\text{H})$ 42 Hz. ^{13}C And $^{117/119}\text{Sn}$ spectra are reported in Table 2.

2,2-Di-*t*-butyl-1,3,2-dithiastannolane

Equimolar amounts of 2,2-dimethyl-1,3,2-dithiastannolane and di-*t*-butyltin oxide (4×10^{-3} mol) were refluxed in benzene for several hours. The dimethyltin oxide which separated was filtered off ($< 95\%$), then the solvent was removed and the product was recrystallised from pentane yielding the dithiastannolane, m.p. 36°C . Found: C, 37.0; H, 6.57; S, 19.6. $\text{C}_{10}\text{H}_{22}\text{S}_2\text{Sn}$ calcd.: C, 37.0; H, 6.82; S, 19.7%. $\delta(^1\text{H})$ (CDCl_3 , 60 MHz); 1.33 (s, 18H, Me), $^3J(^{119}\text{Sn}-\text{H})$ 91 Hz, $^3J(^{117}\text{Sn}-\text{H})$ 87 Hz;

Table 7

Fractional atomic coordinates ($\times 10^4$) for $[\text{Bu}_2\text{SnOCH}_2\text{CH}_2\text{O}]_2$

	x	y	z
Sn(1)	6386.7(3)	4574.6(3)	0
O(11)	4792(3)	4062(3)	0
O(12)	6611(4)	2957(4)	0
C(11)	4707(6)	2933(6)	-178(8)
C(12)	5631(8)	2368(7)	242(8)
C(13)	7127(4)	4905(4)	-1192(3)
C(14)	8293(4)	4545(6)	-1141(4)
C(15)	6553(5)	4242(6)	-1835(4)
C(16)	7083(5)	6070(5)	-1413(4)
Sn(2)	5385.4(3)	1383.1(4)	5000
O(21)	4954(3)	-185(4)	5000
O(22)	7008(4)	1651(5)	5000
C(21)	7090(6)	-258(7)	4836(8)
C(22)	7597(6)	685(8)	5256(7)
C(23)	5034(4)	2109(4)	3811(3)
C(24)	5384(5)	3263(5)	3862(4)
C(25)	5718(6)	1544(5)	3159(4)
C(26)	3859(5)	2039(6)	3580(4)

3.00 (s, 4H, CH₂S), ³J(^{117/119}Sn–H) 30 Hz. The ¹³C and ^{117/119}Sn spectra are reported in Table 2.

X-Ray crystallography

Unit-cell parameters and intensity data were obtained by the previously described procedures [17], using a CAD4 diffractometer operating in the ω - 2θ scan mode, with graphite monochromated Mo- K_{α} radiation (λ 0.71069 Å). The reflection intensities for all three structures were corrected for absorption, using the azimuthal-scan method [18]. The relevant experimental details are summarized in Table 6.

The structures were solved by the application of routine heavy-atom methods (SHELX84 [19]), and refined by full-matrix least-squares (SHELX76 [20]). The final cycles of refinement included hydrogen atoms in their calculated positions (C–H 0.96 Å, U 0.10 Å²)*. All non hydrogen atoms were refined anisotropically. Atomic scattering factors and anomalous scattering parameters were taken from ref. 21 and 22, respectively. All computations were made on a DEC VAX-11/750 computer.

Table 8

Fractional atomic co-ordinates ($\times 10^4$) for [Bu^t₂SnOCH₂CH₂S]₂

	x	y	z
Sn(1)	1404.3(2)	947.5(2)	2111.1(2)
Sn(2)	-1421.6(2)	1677.5(2)	2551.6(2)
S(1)	1523(1)	-623(1)	1620(1)
S(2)	-1589(1)	3263(1)	2992(1)
O(1)	291(3)	2084(2)	2495(2)
O(2)	-325(2)	559(2)	2129(2)
C(1)	223(5)	-982(3)	1968(4)
C(2)	-740(5)	-301(3)	1776(4)
C(3)	14(5)	3454(4)	3230(5)
C(4)	564(5)	3035(3)	2587(4)
C(5)	2740(5)	909(3)	3325(3)
C(6)	1846(5)	1664(4)	1032(4)
C(7)	-2898(5)	1661(4)	1404(3)
C(8)	-1629(5)	1033(4)	3732(3)
C(51)	2333(7)	192(5)	3879(5)
C(52)	2884(7)	1773(5)	3805(5)
C(53)	3888(6)	619(7)	3133(6)
C(61)	2575(8)	2488(5)	1336(5)
C(62)	2625(8)	1041(6)	632(6)
C(63)	724(7)	1876(7)	393(5)
C(71)	-3493(7)	756(5)	1289(6)
C(72)	-3823(6)	2321(6)	1535(6)
C(73)	-2455(9)	1861(12)	670(6)
C(81)	-1426(6)	24(4)	3720(4)
C(82)	-2861(6)	1262(6)	3814(5)
C(83)	-688(6)	1407(5)	4469(4)

* As the chelate ring carbon atoms for the dioxastannolane show disorder about a crystallographic mirror plane (see Fig. 2), their attached hydrogen atoms were not included.

Table 9

Fractional atomic coordinates ($\times 10^4$) for $\text{Bu}_2\text{SnSCH}_2\text{CH}_2\text{S}$

	<i>x</i>	<i>y</i>	<i>z</i>
Sn	71.9(4)	7156.8(2)	3187.0(2)
S(1)	1536(2)	5746(1)	3860(1)
S(2)	-3396(2)	6552(1)	3293(1)
C(1)	-844(7)	5054(4)	3857(4)
C(2)	-2722(7)	5623(4)	4042(4)
C(3)	683(8)	7264(4)	1909(3)
C(4)	2616(11)	7836(6)	1796(4)
C(5)	932(7)	6259(5)	1589(5)
C(6)	-1039(12)	7806(7)	1486(4)
C(7)	508(7)	8444(3)	3936(3)
C(8)	-369(14)	8215(6)	4745(4)
C(9)	-650(11)	9277(4)	3540(4)
C(10)	2790(9)	8681(4)	4046(4)

Atom coordinates are listed in Tables 7–9. Tables of isotropic hydrogen atom coordinates, anisotropic thermal coefficients, and F_o/F_c values have been deposited as supplementary data, and are available on request from the Director of the Cambridge Crystallographic Data Centre, University Chemical Laboratory, Lensfield Road, Cambridge CB2 1EW (U.K.).

Acknowledgements

This work was carried out by Sean Slater during the tenure of an S.E.R.C. C.A.S.E. Studentship in association with the International Tin Research Council. We are grateful to Dr. W.B. Fitzsimmons and W.G. Marshall of Birkbeck College, and Dr. C. Groombridge of Royal Holloway and Bedford New College for their assistance with the Mössbauer spectra and the solid state NMR spectra, respectively.

References

- 1 A.G. Davies and P.W. Smith, in G. Wilkinson, F.G.A. Stone, and E.W. Abel, (Eds.) *Comprehensive Organometallic Chemistry*, Pergamon Press, Oxford, 1982, Vol. 2, p. 519.
- 2 J.A. Zubieta and J.J. Zuckerman, *Prog. Inorg. Chem.*, 24 (1978) 251.
- 3 P.J. Smith, *Organomet. Chem. Rev. A*, 5 (1970) 573.
- 4 J.N.R. Ruddick, *Rev. Silicon, Germanium, Tin, and Lead Compounds*, 2 (1976) 115.
- 5 P.J. Smith and A.P. Tupčiauskas, *Ann. Rev. NMR Spectrosc.*, 8 (1978) 291.
- 6 R.K. Harris, J.D. Kennedy, and W. McFarlane, in R.K. Harris and B.E. Mann (Eds.), *NMR and the Periodic Table*, Academic Press, London, 1978, p. 342.
- 7 P.A. Cusack, P.J. Smith, J.D. Donaldson, and S.M. Grimes, *A Bibliography of X-Ray Crystal Structures of Tin Compounds*, International Tin Research Institute, London, 1981.
- 8 A.G. Davies and S.D. Slater, *Silicon, Germanium, Tin, and Lead Compounds*, 9 (1986) 87.
- 9 A.G. Davies, A.J. Price, H.M. Dawes, and M.B. Hursthouse, *J. Chem. Soc. Dalton Trans.*, (1986) 297.
- 10 P.A. Bates, M.B. Hursthouse, A.G. Davies, and S.D. Slater, *J. Organomet. Chem.*, 325 (1987) 129.
- 11 A.G. Davies, S.D. Slater, D.C. Povey, and G.W. Smith, *J. Organomet. Chem.*, 352 (1988) 283.
- 12 C.W. Holzapfel, J.M. Kockemoer, C.M. Marais, G.J. Kruger, and J.A. Pretorius, *S. Afr. J. Chem.*, 35 (1982) 81.
- 13 S. David, C. Pascard, and M. Cesario, *Nouv. J. Chim.*, 3 (1979) 63.

- 14 M. Drager, *Z. Anorg. Allg. Chem.*, 447 (1981) 154.
- 15 A.S. Secco and J. Trotter, *Acta Crystallogr. C*, 39 (1983) 451.
- 16 A.G. Davies, J.A.-A. Hawari, and Pan Hua-De, *J. Organomet. Chem.*, 241 (1983) 203.
- 17 M.B. Hursthouse, R.A. Jones, K.M.A. Malik, and G. Wilkinson, *J. Am. Chem. Soc.*, 101 (1979) 4128.
- 18 A.C.T. North, D.C. Phillips, and F.S. Mathews, *Acta Crystallogr. A*, 24 (1968) 351.
- 19 G.M. Sheldrick, SHELX84 Program for Crystal Structure Solution, private communication.
- 20 G.M. Sheldrick, SHELX76 Program for Crystal Structure Determination and Refinement, University of Cambridge, 1976.
- 21 D.T. Cromer and J.B. Mann, *Acta Crystallogr. A*, 24 (1968) 321.
- 22 D.T. Cromer and D. Leberman, *J. Chem. Phys.*, 53 (1970) 1891.